

Proximity effects in spin-triplet superconductor-ferromagnet heterostructure with spin-active interface

Damien Terrade,^{1,*} Paola Gentile,² Mario Cuoco,² and Dirk Manske¹

¹*Max Planck Institute for Solid State Research, D-70569 Stuttgart, Germany*

²*CNR-SPIN, Fisciano (Salerno), Italy and Dipartimento di Fisica "E.R. Caianiello", Università di Salerno, Fisciano (Salerno)*

(Dated: September 6, 2021)

We study the physical properties of a ballistic heterostructure made of a ferromagnet (FM) and a spin-triplet superconductor (TSC) with a layered structure stacking along the direction perpendicular to the planes where a chiral $p_x + ip_y$ pairing occurs and assuming spin dependent processes at the interface. We use a self-consistent Bogoliubov-de Gennes approach on a three-dimensional lattice to obtain the spatial profiles of the pairing amplitude and the magnetization. We find that, depending on the strength of the ferromagnetic exchange field, the ground state of the system can have two distinct configurations with a parallel or anti-parallel collinearity between the magnetic moments in the bulk and at the interface. We demonstrate that a magnetic state having non coplanar interface, bulk and Cooper pairs spins may be stabilized if the bulk magnetization is assumed to be fixed along a given direction. The study of the density of states reveals that the modification of the electronic spectrum in the FM plays an important role in the setting of the optimal magnetic configuration. Finally, we find the existence of induced spin-polarized pair correlations in the FM-TSC system.

PACS numbers: 74.45.+c, 74.20.Rp, 74.50.+r

I. INTRODUCTION

The past few decades have been marked by a growing interest in the study of the interplay between superconductivity and ferromagnetism in heterostructures both for the potential application in the field of spintronics and because of the underlying fundamental physics¹⁻⁴. The control of the spin degree of freedom in charge currents that can flow without dissipation represents one of the major challenges in the context of hybrids based on superconductors and ferromagnets. In this respect, the presence of spin-triplet pair correlations in ferromagnet(FM)-superconductor(SC) heterostructures is expected to play a key role in the generation of new types of spin-valves or unconventional Josephson junctions.

One of the major obstacle to such achievement is the difficulty in obtaining a coexistence of superconductivity and ferromagnetism within a uniform quantum state. The competition between the two orders can be reduced by a phase or amplitude modulation of the superconductor order parameter, as for the so called Fulde-Ferrell-Larkin-Ovchinnikov (FFLO) state⁵, by having ferromagnetic domains with no net magnetization in average on the scale of the superconducting coherence length, or via specific mechanisms driving the ferromagnetism⁶. Such incompatibility, due to the opposite nature of the order parameters, gets less severe in a ferromagnet- spin-singlet superconductor (SSC) heterostructure through the occurrence of nanoscale proximity effects at the interfaces. One remarkable feature due to the proximity effects is an induced pairing amplitude in the ferromagnet, characterized by a damped oscillatory behaviour⁷⁻⁹. This leads to a nonmonotonous dependence of the superconducting critical temperature as well as a $0-\pi$ transition in the Josephson current and the possibility to suppress the su-

perconductivity according to the FM thickness^{2,10,11,13}. Moreover, spin-triplet pair correlations being even in space and odd in time or frequency can also be induced in the presence of magnetic inhomogeneities and significantly contribute in the spin polarized supercurrent¹⁴⁻²². Experimental evidence for such odd-in-time spin-triplet pairs was accomplished either by introducing magnetic inhomogeneity artificially, or by relying on a source of inhomogeneity intrinsic to the materials in SC-FM-SC Josephson junctions²³⁻²⁹. Non uniform magnetic configurations can be intrinsic or artificially designed, as for instance in the case of a FM1-FM2-SSC heterostructure with noncollinear magnetization between FM1 and FM2 ferromagnets. The FM2 ferromagnet acts in this configuration as a spin-active interface where its magnetization orientation with respect to the FM1 magnetization is the key parameter to tune the proximity effects³⁰. In turn the presence of the FM2 layer results into a change of the pair-breaking intensity and of the superconducting critical temperature. Both the proximity effects and the induced spin-triplet pairing can contribute to generate a spin-valve effect by turning the superconductivity on and off depending on the pattern of the magnetic profile³¹⁻³⁴.

Differently from the induced triplet correlations, a spin-triplet superconductor (TSC) is marked by a broken symmetry configuration due to a characteristic pairing potential. Spin-triplet superconducting order has been predicted in systems like the heavy-fermion compounds UPt_3 ³⁵ and UGe_2 ³⁶, the quasi-one-dimensional organic Bechgaard salts $(TMTSF)_2X$ ³⁷, and the perovskite ruthenium oxide Sr_2RuO_4 ³⁸. While in the first two cases a non-unitary pairing seems to occur, a unitary chiral-state where time-reversal symmetry is broken by orbital degrees of freedom is realized in the latter³⁹. A peculiarity of this state is its non-trivial topological character, specified by a fully open excitation en-

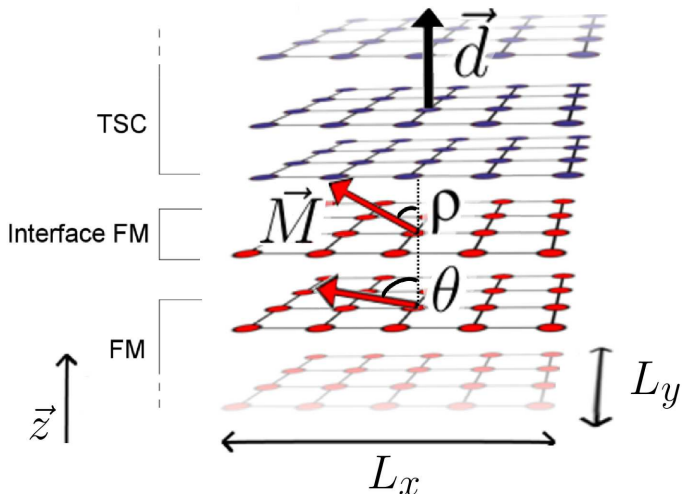


FIG. 1. (color online) FM-TSC heterostructure with the interface perpendicular to the z -direction. The blue layers are for the spin-triplet superconductor with a \vec{d} -vector (thick black arrow) perpendicular to the (xy) -plane and the red layers indicate the ferromagnetic region. The red thin arrow stands for the magnetization \vec{M} in the interior of the ferromagnetic region (at the interface), due to the exchange field forming a relative angle θ (ρ) with respect to the \vec{d} -vector. L_x and L_y are the in-plane lateral size of the heterostructure.

ergy gap coexisting with topologically protected gapless edge states. Spin-triplet pairing may also manifest itself in non-centrosymmetric superconductors (NCS)^{40,41} together with the spin-singlet component, due to the lack of a crystal inversion center that leads to an asymmetric spin-orbit interaction and in turn results into parity mixing⁴². The increasing number of materials having a superconducting order parameter with a spin-triplet symmetry makes more achievable the design of TSC based heterostructures. In particular the recent preparation⁴³ of superconducting thin films of Sr_2RuO_4 ⁴⁴ provides a key milestone for the development of such hybrid systems. Within this context the epitaxial growth of the cubic itinerant ferromagnet SrRuO_3 on the top of Sr_2RuO_4 could allow one to obtain an FM-TSC heterostructure with the desired control of the interface.

The physical behaviour of the FM-TSC heterostructure is expected to be quite different from that of the FM-SSC. This is especially due to the basic different structure of the spin-triplet order parameter that has a vectorial nature and thus can couple to the orientation of the FM moment as well as to the orbital one. Such features play a distinct role in controlling the dependence of the proximity effects in TSC-FM bilayers with diffusive FM⁴⁵ and the sign of the current in TSC-FM-TSC Josephson junctions⁴⁶. The interface with the FM also induces specific effects in the TSC generating a Josephson-like coupling between the spin \uparrow and \downarrow condensates of the TSC^{47,48}.

Furthermore, in a FM-TSC heterostructure with a planar geometry the ferromagnet magnetization tends to favor a specific orientation in a way that depends on the orbital symmetry of the order parameter rather than that of the Cooper pairs spin⁴⁹. The role of spin-misalignment on hybrids based on TSC, in analogy with the FM1-FM2-SSC systems, can significantly modify the above scenario and yield novel physical behaviors. So far it has been considered only for the case of a half-metal ferromagnet demonstrating that extra midgap states can be induced as well as a nonzero charge conductance⁵⁰.

In this paper we aim to study the role of *spin-dependent* interface processes in determining the proximity effects and the physical properties of an FM-TSC heterostructure. In particular, we consider FM and TSC layers stacked along the z -direction perpendicular to the plane where a chiral $p_x + ip_y$ pairing occurs in the TSC and with a spin-active interface such as to mimic an FM1-FM2-TSC heterostructure (see Fig. 1). We employ a fully self-consistent Bogoliubov-de Gennes approach on a lattice to determine the proximity behaviour through the spatial profile of the spin-triplet pair amplitude and the magnetization. We obtain the optimal orientation of the magnetization, for the bulk and the interface, in the presence of the spin-triplet superconductor. We found that the optimal configuration is highly depending on the strength of the ferromagnetic exchange field. While the ground state of the ferromagnet-normal interface can exhibit two distinct magnetic configurations, with spin isotropic parallel or antiparallel magnetic moments among the interface and the interior of the ferromagnet, the presence of the triplet superconductor favors the anti-parallel configuration with in-plane magnetization and can lead to the emergence of a magnetic bulk-interface noncollinearity. This misalignment tunes the coupling between ferromagnetism and superconductivity by leading to a competition between the energy contributions associated with the proximity effects and with the superconducting order parameter and those arising from the energy spectrum reconstruction at the interface. We determine the phase diagram with respect to the most favorable magnetic orientation and discuss the microscopic mechanisms that control the settling of the magnetic configuration. Finally, we discuss how spin-polarized pair correlations are induced in the FM and at the FM-TSC interface depending on the magnetization orientation in the ferromagnet with respect to the direction of the Cooper pairs spin. We believe that the study of such a geometric configuration has a relevant impact in view of a possible application to a Sr_2RuO_4 heterostructure stacked along the c -axis.

The paper is organized as follows. In the Sect. II we introduce the model Hamiltonian and the relevant physical quantities to be determined. The Sect. III and the Sect. IV are devoted to the proximity effects in the FM-TSC and FM₁-FM₂-TSC systems respectively. In the Sect. V we analyze the spin-polarized pair correlations while a qualitative physical scenario is presented in the

Sect. VI. Finally, the concluding remarks are provided in the Sect. VII.

II. THE MODEL

We consider a FM-TSC heterostructure with a layered geometry (see Fig. 1) described by a single-band tight-binding model Hamiltonian with an in-plane attractive nearest-neighbor interaction such as to yield a spin-triplet pairing with chiral symmetry in the superconducting side. In the framework of an effective Stoner model for itinerant magnets, an exchange field h (h_{int}) is introduced to yield a nonzero spin polarization in the ferromagnetic layers (at the interfacial layer with the TSC). Denoting by z and $\{x, y\}$ the directions perpendicular and parallel to the interface layer, respectively, we assume that the system is uniform along the x and y axes, so that the translational symmetry is broken only in the z direction. The total Hamiltonian of the system is then defined on a lattice with size $L_x \times L_y \times L_z$ ($L_x = L_y = L$) with periodic boundary conditions along x and y . The simulation is performed for a system size with $L = 40$ and $L_z = 40$. We indicate each site by a vector $\vec{i} \equiv (i, i_z)$, with i labeling the (xy) in-plane atomic positions and i_z the different layers along the z -direction. The spin-active layer is placed at the site $i_z = 0$ between the FM region ($i_z \leq 0$) and the TSC one ($i_z > 0$). The hopping amplitude is given by $t_x = t_y = t$ for the in-plane processes and $t_z = t/2$ uniformly for all the inter-layers charge transfer, including that at the FM-TSC interface. A different choice of the single particle electronic parameters and the system size alters only quantitatively and not qualitatively the presented results. All the energy scales are in unit of t and for clarity, the exchange fields have been scaled with respect to the amplitude $h_{\text{HM}} = 3.15 t$ corresponding to the ferromagnetic half-metallic state, i.e. when there is only one type of carriers at the Fermi level and the minority spin electrons have a gap in the excitation spectrum. With the above assumptions the Hamiltonian can be expressed as

$$\begin{aligned}
 H = & \sum_{k, i_z, \sigma} (\epsilon_{k\sigma} - \mu) c_{k\sigma}^\dagger(i_z) c_{k\sigma}(i_z) + \\
 & - \sum_{\langle ij \rangle, i_z > 0} V [n_{i\uparrow}(i_z) n_{j\downarrow}(i_z) + n_{i\downarrow}(i_z) n_{j\uparrow}(i_z)] \\
 & + \sum_{\delta=\pm 1} \sum_{k\sigma} t_z (c_{k\sigma}^\dagger(i_z + \delta) c_{k\sigma}(i_z) + h.c.) + \\
 & - \sum_{i_z < 0} \vec{h} \cdot \vec{s}(i_z) - \vec{h}_{\text{int}} \cdot \vec{s}(0)
 \end{aligned} \quad (1)$$

with $c_{k\sigma}(i_z)$ being the annihilation operator of an electron with planar momentum k , spin σ at the layer i_z and where $\langle ij \rangle$ denotes the in-plane nearest-neighbor sites, μ is the chemical potential and V is the in-plane pairing strength. Moreover $\vec{s}(i_z) = \sum_{i, s, s'} c_{i, s}^\dagger(i_z) \vec{\sigma}_{s, s'} c_{i, s'}(i_z)$ is the spin density of

the layer i_z , and $\epsilon_{k\sigma} = -2t[\cos(k_x) + \cos(k_y)]$ is the in-plane tight-binding spectrum.

For the analysis of the proximity effects and of the most energetically favorable magnetic configurations the quartic term of the model Hamiltonian in Eq. 1 is decoupled in the Hartree-Fock approximation within the pairing channel. We introduce the pairing amplitude for an in-plane bond $F_{ij}(i_z) = \langle c_{i\uparrow}(i_z) c_{j\downarrow}(i_z) \rangle$ at a given layer i_z . The average $\langle A \rangle$ indicates the thermal expectation value of the operator A . Within such decoupling scheme, the Hartree-Fock Hamiltonian is

$$\begin{aligned}
 H_{\text{HF}} = & \sum_{k, i_z, \sigma} (\epsilon_{k\sigma} - \mu) c_{k\sigma}^\dagger(i_z) c_{k\sigma}(i_z) + \\
 & + \sum_{\langle ij \rangle, i_z > 0} V \left[F_{ij}(i_z) c_{j\downarrow}^\dagger(i_z) c_{i\uparrow}^\dagger(i_z) \right. \\
 & + \left. F_{ji}(i_z) c_{i\downarrow}^\dagger(i_z) c_{j\uparrow}^\dagger(i_z) + h.c. \right] \\
 & + \sum_{\delta=\pm 1} \sum_{k\sigma} t_z (c_{k\sigma}^\dagger(i_z + \delta) c_{k\sigma}(i_z) + h.c.) + \\
 & - \sum_{i_z < 0} \vec{h} \cdot \vec{s}(i_z) - \vec{h}_{\text{int}} \cdot \vec{s}(0).
 \end{aligned} \quad (2)$$

From the pairing amplitude $F_{ij}(i_z)$ it is possible to build up the superconducting order parameter with the desired symmetry, to be then determined self-consistently^{51,52}. By a proper selection of the spin-triplet channel one can derive the pairing amplitude for each layer by summing up the contributions over all the in-plane k vectors.

In general, for a spin-triplet superconductor the order parameter can be expressed in a matrix form as

$$\Delta(k) = \begin{pmatrix} \Delta_{\uparrow\uparrow}(k) & \Delta_{\uparrow\downarrow}(k) \\ \Delta_{\downarrow\uparrow}(k) & \Delta_{\downarrow\downarrow}(k) \end{pmatrix} = \begin{pmatrix} -d_x + id_y & d_z \\ d_z & d_x + id_y \end{pmatrix},$$

where the \vec{d} -vector components are related to the pair correlations of the various spin-triplet configurations. Indeed, $d_x = \frac{1}{2}(-\Delta_{\uparrow\uparrow}(k) + \Delta_{\downarrow\downarrow}(k))$, $d_y = \frac{1}{2i}(\Delta_{\uparrow\uparrow}(k) + \Delta_{\downarrow\downarrow}(k))$, and $d_z = \Delta_{\uparrow\downarrow}(k)$ are expressed in terms of the equal spin $\Delta_{\uparrow\uparrow}(k)$ and $\Delta_{\downarrow\downarrow}(k)$, and the anti-aligned spin $\Delta_{\uparrow\downarrow}(k)$ pair potentials. For the model upon examination the pairing interaction V is non zero in the $\uparrow\downarrow$ channel and thus the only non-vanishing order parameter is $\Delta_{\uparrow\downarrow}(k)$. This implies that the \vec{d} -vector is oriented along the z -direction, which is chosen to be perpendicular to the layers as indicated in Fig. 1.

It is worth pointing out that since we are dealing with a hybrid structure where the superconductor is interfaced to a ferromagnet, the spin-triplet pair correlations can have also contributions in the $\uparrow\uparrow$ and $\downarrow\downarrow$ channels. For this reason it is useful to introduce the following pair

correlators

$$F_{p_\alpha}(i_z) = \frac{1}{L_x L_y} \sum_k \sin(k_\alpha) \langle c_{k\uparrow}(i_z) c_{-k\downarrow}(i_z) \rangle \quad (3)$$

$$F_{p_\alpha}^{\sigma\sigma}(i_z) = \frac{1}{L_x L_y} \sum_k \sin(k_\alpha) \langle c_{k\sigma}(i_z) c_{-k\sigma}(i_z) \rangle \quad (4)$$

with $\alpha = x, y$ and $\sigma = \uparrow, \downarrow$.

The analysis is performed by choosing the chemical potential ($\mu = -1.8t$) such that the most stable superconducting state manifests a chiral $p_x + ip_y$ symmetry. This is a stable state for the chosen chemical potential and holds for all the values of V^{53} . In general, for the examined model Hamiltonian, there is a competition between the spin-triplet state and different types of spin-singlet pairing functions, i.e. d -wave and extended s -wave, as a function of temperature and chemical potential. However the chiral spin triplet is more stable than the spin-singlet ones for a suitable window of chemical potential values, i.e. about $-1.5 < \mu < 2.25$. This is because the Fermi surface gets closer to the points $(\pm\pi/2, \pm\pi/2)$ and therefore the k -dependent pairing potential, being proportional to $(\sin(k_x), \sin(k_y))$, can be maximized there. In order to assess the role of the pairing strength in the interplay between superconductivity and ferromagnetism we have also considered different values of the pairing interaction. We point out that the pairing develops in the xy plane and thus a modification of its strength has a consequence on the amplitude of the order parameter and the planar coherence length, while it weakly affects the pair correlations length along the out-of-plane direction.

Concerning the ferromagnetic side of the heterostructure the inner layers magnetization \vec{M} depends on the exchange field \vec{h} , directly proportional to \vec{M} , and its orientation is given by fixing the angle θ with respect to the direction of the \vec{d} -vector (Fig. 1). On the other hand, the interface exchange field \vec{h}_{int} , forming an angle ρ with respect to the \vec{d} -vector, is used to control the interface magnetic moment (Fig. 1). The angle θ and ρ are treated as variational parameters. Due to the rotational spin symmetry of the superconducting state, the x - and y -directions are equivalent. Hence, we can consider \vec{h} to lie in the (xz) -plane with components given by $\vec{h} = h(\sin(\theta), 0, \cos(\theta))$ and similarly for $\vec{h}_{\text{int}} = h_{\text{int}}(\sin(\rho), 0, \cos(\rho))$.

After having diagonalized the Hartree-Fock Hamiltonian H_{HF} (Eq.(2)), the Gibbs free energy can be determined as

$$G = -\frac{1}{\beta} \ln \text{Tr}[e^{-\beta H_{\text{HF}}}] \quad (5)$$

where $\beta = \frac{1}{k_B T}$ is the inverse temperature, k_B being the Boltzmann constant. In order to separate the energy contributions resulting from the proximity effects and from the modification of the energy spectrum by those that

enters in the superconducting condensation energy, via the change of the order parameter in the TSC side of the heterostructure, it is useful to introduce the quantity E_{op} expressed as

$$E_{\text{op}} = -\left(\frac{2}{L_z}\right) \sum_{i_z > 0} [|F_{p_x}(i_z)|^2 + |F_{p_y}(i_z)|^2] \quad (6)$$

Such quantity reflects the changes of the superconducting order parameter in the FM-TSC heterostructure related to the magnetization configuration of the ferromagnetic layers. In particular, a minimum in E_{op} implies a maximum amplitude of the superconducting order parameter.

Furthermore, for clarity the results are presented by rescaling the Gibbs free energy and the order-parameter derived energy to their minimum value. Indeed, we introduce the quantities $\Delta G = G - G^{\text{min}}$ and $\Delta E_{\text{op}} = E_{\text{op}} - E_{\text{op}}^{\text{min}}$ where G^{min} and $E_{\text{op}}^{\text{min}}$ are the minimum amplitude of the Gibbs energy and of the order parameter energy, respectively, in the analyzed range of parameters. This rescaling allows one to directly extract the energy scale that sets the variation of the Gibbs energy landscape and to compare different energy profiles as a function of the physical parameters involved in the analysis. Still, the variation of ΔG and ΔE_{op} are presented by scaling their amplitude to the value of E_{op} associated with a single superconducting layer in the homogenous state.

III. PROXIMITY EFFECTS AND OPTIMAL MAGNETIC CONFIGURATION OF FM-TSC SYSTEM

In this section we present the evolution of the pairing amplitude of the FM-TSC system assuming that the ferromagnet has a uniform magnetization i.e., $\theta = \rho$.

To analyze the most stable magnetic configurations we firstly study the modification of the pairing amplitude as a function of the relative angle between the exchange fields and the \vec{d} -vector. As depicted in Fig. 2 the spatial dependence of the real part of the pairing amplitude for the p_x component has a distinct behavior with respect to the angle θ when considering the FM and the TSC side of the heterostructure. The imaginary part of the p_y component exhibits the same behaviour of the p_x counterpart due to the tetragonal symmetry of the system. In the TSC region the pairing amplitude is reduced close to the interface, with a maximum reduction for $\theta = 0$ (see the inset of Fig. 2). The main outcome of this analysis is that the pairing amplitude has a monotonous dependence on the angle θ and it reaches its maximum when the magnetization is aligned in-plane perpendicularly to the \vec{d} -vector.

On the other hand in the FM side the pairing amplitude exhibits a spatial damped oscillatory behavior at any angle $\theta \neq \pi/2$ and a pure monotonous dependence

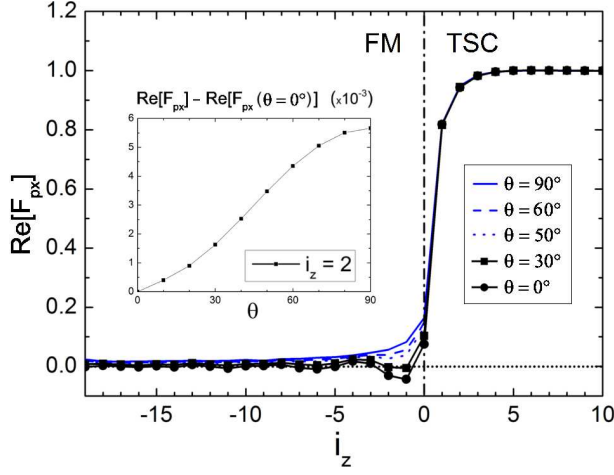


FIG. 2. (color online) Spatial variation of the real part of the p_x -wave pairing amplitude F_{p_x} scaled to the TSC bulk value for various angles θ of the exchange field with respect to the \vec{d} -vector as defined in Fig. 1. For this case we assume $h = h_{\text{int}} = 0.16$ and $\theta = \rho$. The FM-TSC interface ($i_z = 0$) is denoted by the dashed line. The inset shows the evolution of the pairing amplitude F_{p_x} as a function of the angle θ at a given layer $i_z = 2$.

when the magnetization is perpendicular to the \vec{d} -vector. The oscillatory behaviour of the pairing amplitude comes from the spin pair-breaking effect of the ferromagnet. Indeed, the Cooper pairs spin is perpendicular to the \vec{d} -vector, and therefore the only non pair-breaking configuration for the superconducting components within the ferromagnet happens when $\theta = \pi/2$.

Moreover, the oscillation length does not depend on θ because the split of the energy for the up and down electrons, that controls the modulation in the proximity, is always proportional to the amplitude of the ferromagnetic exchange field h and not on the pair-breaking projection. It is worth pointing out that differently from the SSC junction, the oscillation of the pairing amplitude leads to a negative phase shift only for a value of θ in the range $\sim [0, \pi/4]$. Still, we note that in this case there are no spin singlet induced components at the interface differently to what is observed in a planar FM-TSC heterostructures where the interface explicitly breaks the inversion symmetry in the spatial directions that enter into the spin-triplet order parameter⁵².

We are now interested in the energetically most favorable magnetization orientation in the ferromagnetic layers. We have analyzed the evolution of the Gibbs free energy G and of the energy associated with the TSC order parameter E_{op} for different values of the relative orientation of the ferromagnetic moment with respect to the \vec{d} -vector and as a function of the strength of the ferromagnetic exchange field.

As one can note in the Fig. 3 the Gibbs free energy has

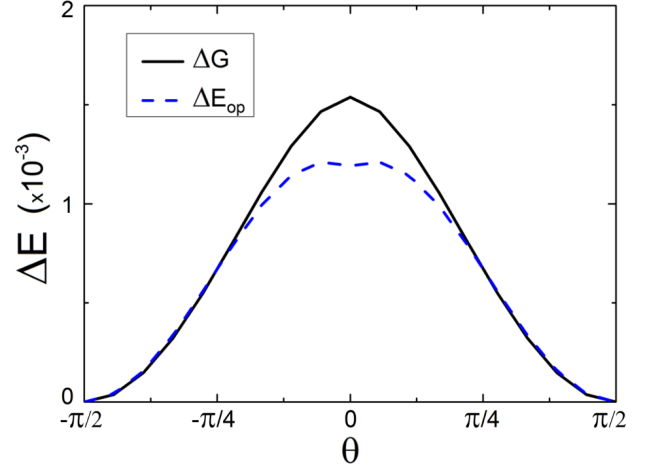


FIG. 3. (color online) variation of the Gibbs free energy (solid black line) and the order-parameter derived energy E_{op} (blue dotted line) as functions of the angle θ at a given value of the ferromagnetic exchange $h = 0.32$. Both energies are scaled with respect to their minimum amplitude ($\Delta G = G - G^{\text{min}}$ and $\Delta E_{\text{op}} = E_{\text{op}} - E_{\text{op}}^{\text{min}}$) and are renormalized to the E_{op} value of a single superconducting layer in the homogenous state.

a non monotonous profile with two degenerate minima at $\theta = \pm\pi/2$ and a maximum for $\theta = 0$. This means that, due to the coupling with the TSC, the energetically most favorable magnetic configuration for the ferromagnet is achieved when the magnetization lies in the plane of the Cooper pairs spin. Otherwise, the maximal loss in the energy occurs when the magnetization is parallel to the \vec{d} -vector. To understand the driving force in the stability of the magnetic configuration it is instructive to analyze the behavior of the order-parameter derived energy E_{op} . The results indicate that the maximum energy gain due to the variation of the superconducting order parameter in the TSC region occurs for a magnetization that lies perpendicular to the \vec{d} -vector which also corresponds to a lack of spin-pair breaking in the proximity effect. Since the total energy has the same minima than the E_{op} term one can deduce that for this strength of the exchange field the changes of the spectra in the Gibbs free energy due to the proximity effect and to a possible electronic reconstruction at the interface cooperate with the gain in the condensation energy to stabilize the observed magnetic configuration.

The trend observed for the pairing amplitude as a function of the angle θ can be discussed in the framework of the scattering formulation for the TSC-FM heterostructure. The pairing amplitude variation is mainly controlled by the Andreev reflections at the interface. Since Andreev scattered electron (hole) leads to hole (electron) pairs formation in the superconductor such process is expected to drive the change of the pairing order parameter close to the interface. The resulting interference of the different scattering amplitude is maximal when the An-

dreiev reflected Cooper pair acquires a spin and/or an orbital phase shift^{47–49,54}. This observation can be justified by the fact that a sign change can lead to destructive interference. In the case upon examination in the paper, the orbital phase change for the given heterostructure is 0 at any angle of incidence of the electron that undergoes an Andreev reflection and therefore the overall phase shift is minimized when the magnetization forms an angle $\pi/2$ with the \vec{d} -vector⁴⁷.

IV. SPIN-ACTIVE PROCESSES AT FM-TSC INTERFACE

In this section we analyze the role of spin-dependent processes at the FM-TSC interface with the aim to find the most favorable magnetic orientation in the presence of an extra degree of freedom for the spin moments at the interface. Concerning the modification of the pairing amplitude in the TSC, the presence of a spin-scattering interface does not modify substantially the trend observed for the uniform case with $\theta = \rho$. Indeed, the TSC order parameter is maximized when both the magnetization at the interface and in the bulk lies in the plane perpendicular to the \vec{d} -vector. More specifically, when restricting the magnetic orientation to the xy -plane, we find that the pairing amplitude in the TSC region increases for θ and ρ being collinear and antiparallel. The behaviour in the FM region shows that the intensity of the pairing amplitude has an oscillatory/monotonous profile similar to the case with uniform magnetization. Nevertheless, for the planar orientations it turns out to be larger for the parallel interface-bulk configuration if compared to the antiparallel one. This implies a reduction of the proximity effect when the bulk-interface magnetic moments are antiparallel aligned.

A. Optimal magnetic configuration

The analysis of the energies variations reveals a complex scenario because the presence of spin-dependent processes at the interface tends to modify the balance in the Gibbs free energy due to the electronic spectrum and to the superconducting order parameter. In the following we consider two possible physical situations for the search of the most favorable magnetic configuration: i) the magnetization in the bulk and at the interface of the FM have no preferential orientation (i.e. θ and ρ are treated as independent variational parameters), ii) the magnetization in the bulk is fixed in amplitude and orientation (for instance due to an intrinsic source of magnetic anisotropy or is pinned externally along a specific direction via an exchange-bias coupling) and we look for the optimal orientation of the magnetization at the interface which minimizes the Gibbs free energy. For both cases the amplitude of the spin moments is chosen by fixing

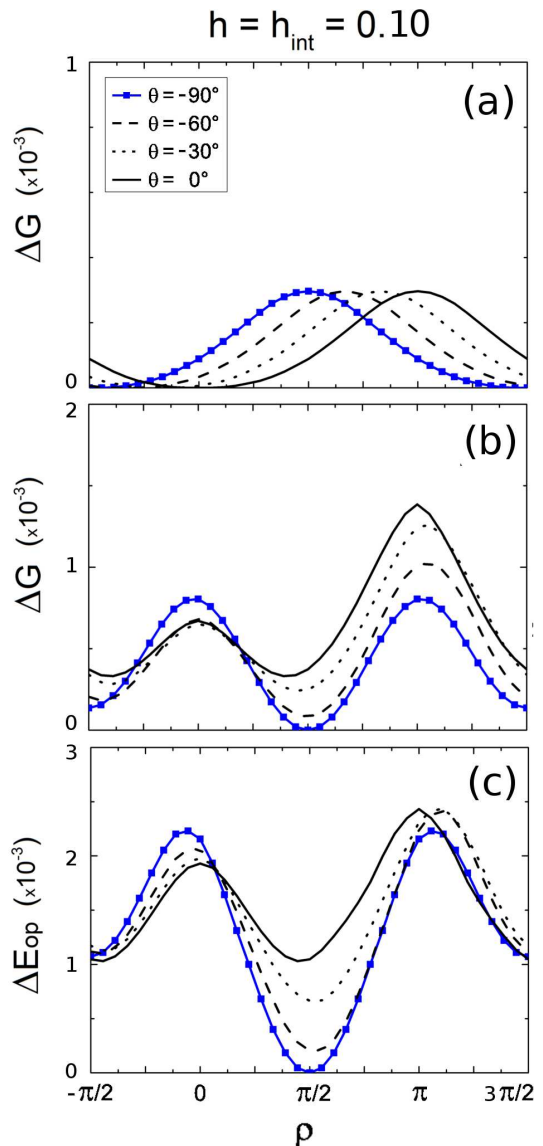


FIG. 4. (color online) Variation of the Gibbs free energy for $V=0.0t$ (a) and $V=-2.0t$ (b), scaled with respect to its minimum amplitude G^{\min} ($\Delta G = G - G^{\min}$) and renormalized to the energy E_{op} associated with a single superconducting layer in the homogenous case, as a function of the angle ρ at various angle θ and for a given value of the ferromagnetic exchange field $h = h_{\text{int}} = 0.1$. c) Variation of E_{op} ($\Delta E_{op} = E_{op} - E_{op}^{\min}$) energy associated with the superconducting order parameter in the TSC region with the same renormalization and parameters as in a).

the value of the ferromagnetic exchange field h and h_{int} in the bulk FM layers and at the interface, respectively. The behavior of the Gibbs free energy G and the order-parameter derived energy E_{op} with respect to the angles ρ and θ are reported in the Figs. 4, 5 and 6 for which $h = h_{\text{int}} = 0.10, 0.48$, and 0.81 , respectively, are representative values for the regimes of weak, intermediate and strong ferromagnet. The amplitude of the exchange fields

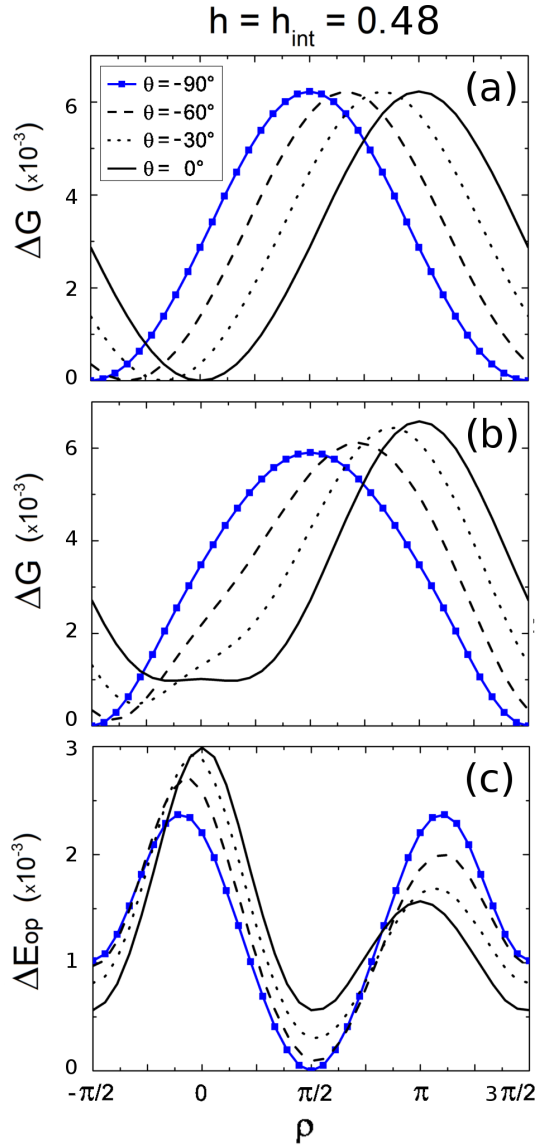


FIG. 5. (color online) Variation of the Gibbs free energy for $V=0.0t$ (a) and $V=-2.0t$ (b), scaled with respect to its minimum amplitude G^{min} ($\Delta G = G - G^{\text{min}}$) and renormalized to the energy E_{op} associated with a single superconducting layer in the homogenous case, as a function of the angle ρ at various angle θ and for a given value of the ferromagnetic exchange field $h = h_{\text{int}} = 0.48$. c) Variation of E_{op} ($\Delta E_{\text{op}} = E_{\text{op}} - E_{\text{op}}^{\text{min}}$) energy associated with the superconducting order parameter in the TSC region with the same renormalization and parameters as in a).

are scaled in such a way that $h = 1$ corresponds to the transition into the half-metallic state with an energy gap in the minority spin band. Furthermore, in order to single out the role of the superconductivity in the energy competition, we have also analyzed the ferromagnet-normal metal (FM-N) heterostructure assuming the same microscopic descriptions of the FM-TSC system with zero pairing interaction V .

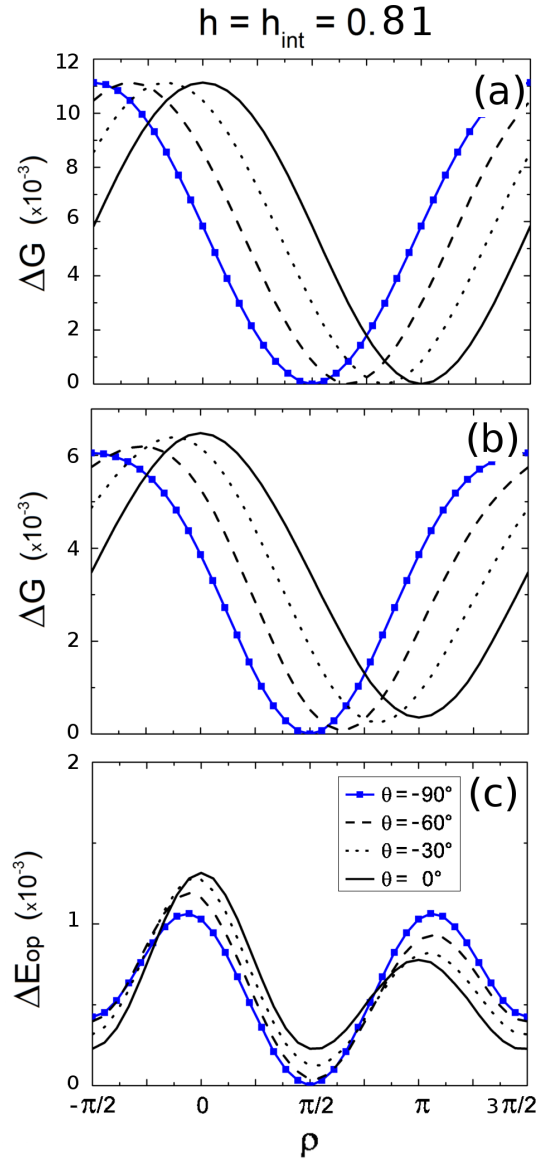


FIG. 6. (color online) Variation of the Gibbs free energy for $V=0.0$ (a) and $V=-2.0t$ (b), scaled with respect to its minimum amplitude G^{min} ($\Delta G = G - G^{\text{min}}$) and renormalized to the energy E_{op} associated with a single superconducting layer in the homogenous case, as a function of the angle ρ at various angles θ and for a given value of the ferromagnetic exchange field $h = h_{\text{int}} = 0.81$. c) Variation of E_{op} ($\Delta E_{\text{op}} = E_{\text{op}} - E_{\text{op}}^{\text{min}}$) energy associated with the superconducting order parameter in the TSC region with the same renormalization and parameters as in a).

Let us start by the FM-N heterostructure. The evolution of the ferromagnetic state can be monitored in the Figs. 4(a), 5(a) and 6(a). For the weak and intermediate ferromagnetic cases, i.e. Figs. 4(a) and 5(a), the minimum of the Gibbs potential corresponds with the configuration where the magnetization in the bulk is parallel to the one at the interface (i.e. $\rho = \theta$, Fig. 7 (a)). Since we

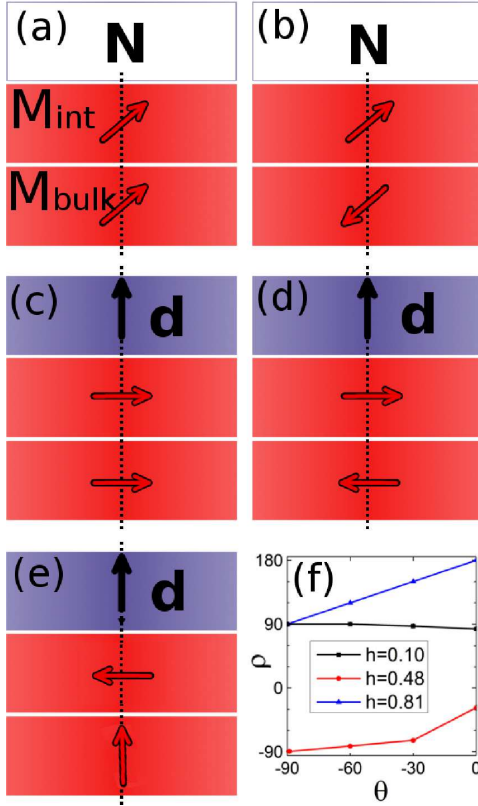


FIG. 7. (color online) Isotropic parallel (a) and antiparallel (b) configurations for a FM/N interface. Parallel (c) and antiparallel (d) configurations in the xy plane for a FM/TSC interface. e) Configuration when the magnetization in the bulk is fixed out of plane. f) Magnetization angle at the interface ρ_{\min} which minimize the free energy for a fixed magnetization angle θ in the bulk.

are describing a ferromagnet without spin anisotropy one finds, as expected, a complete degeneracy in energy for all the possible spin orientations, i.e. the ground state, as expected, is rotational invariant in the spin space. The increase of the ferromagnetic exchange field towards the half-metallic state brings the ground state to have a transition into a different configuration. As one can note by inspection of the Fig. 6(a), the minimum of the Gibbs energy occurs at angles where the magnetization in the bulk and at the interface are antiparallel aligned (i.e. $\rho = -\theta$, Fig. 7 (b)). As for the previous cases the spin invariance is kept and we find that the ground state is degenerate at all the possible orientations of the ferromagnetic magnetization.

When considering the physical case i) where all the magnetic orientations are assumed to be equivalent within the FM, the presence of the spin-triplet superconductor can lead to a breaking of the rotational symmetry for both the magnetic state in the bulk and at the interface. In this circumstance, since θ and ρ are taken as independent variational parameters, it is the absolute minimum of the Gibbs free energy to indicate the most favor-

able magnetic configuration for the FM-TSC system in the presence of spin-dependent processes at the interface. By inspection of Figs. 4(b) and 5(b) one can observe that for $h = h_{\text{int}} = 0.10$ and 0.48 the ground state corresponds to a configuration with parallel interface-bulk magnetic moments, i.e. $\theta = \pi/2$ and $\rho = \pi/2$, with the magnetization lying in the (xy) -plane perpendicular to the \vec{d} -vector (Fig. 7 (c)). However, for $h = h_{\text{int}} = 0.81$ (Fig. 6 (b)) the Gibbs free energy is minimized by an antiparallel configuration within the (xy) -plane i.e., $\theta = \pi/2$ and $\rho = -\pi/2$ (Fig. 7 (d)). The behavior of the order-parameter derived energy, as presented in Figs. 4(c), 5(c) and 6(c), shows that the maximum gain in E_{op} always occurs for an antiparallel interface-bulk configuration.

Moving to the physical case ii) where the exchange field orientation in the bulk FM is kept fixed while it can vary at the interface, all the curves of the Gibbs free energy as a function of ρ at a given angle θ have to be considered separately in order to determine the ground state configuration. The resulting outcome is that for weak and intermediate ferromagnets the minimum of the Gibbs energy is not anymore achieved when the magnetization in the bulk and at the interface are aligned, while an antiparallel configuration remains favorable for any angle θ in the case of a strong ferromagnet. The magnetic configuration at the interface is therefore strongly related to the strength of the ferromagnetic exchange field (see Fig. 7 (f)). More precisely, the most favorable configuration for a weak ferromagnet is with a magnetic orientation at the interface that lies in the plane perpendicular to the \vec{d} -vector almost independently of the magnetic configuration in the bulk. The Fig. 7 (e) represents for example the case where the magnetization in the bulk is pinned perpendicular to the plane, i.e. $\theta = 0$. This means that the superconducting correlations dominate in the scattering processes and in the energy balance. By increasing the amplitude of the ferromagnetic exchange field, the correlation between the magnetization at the interface and that in the bulk is modified in a way that the resulting ground state has a non collinear magnetic profile. The optimal magnetic orientation at the interface clearly exhibits a competition between two effects. We anticipate that this is due to the competition between scattering processes associated with the *normal* and the Andreev reflected electrons. On one side the scattering of the electrons with energies above the superconducting gap would tend to align the bulk and interface magnetization in a parallel configuration, on the other hand the Andreev reflected electrons occurring at midgap energies favor an antiparallel magnetic state with planar spin orientation. The resulting effect is to develop a magnetic interface state with components both along the bulk spin direction and in the plane perpendicular to the \vec{d} -vector. For the considered cases $h = 0.48$ and 0.82 , the deviation from having $\rho = \theta$ is due to the presence of the superconducting processes which always prefers to stabilize an in-plane magnetic orientation.

Indeed, if we look more specifically at the case $h =$

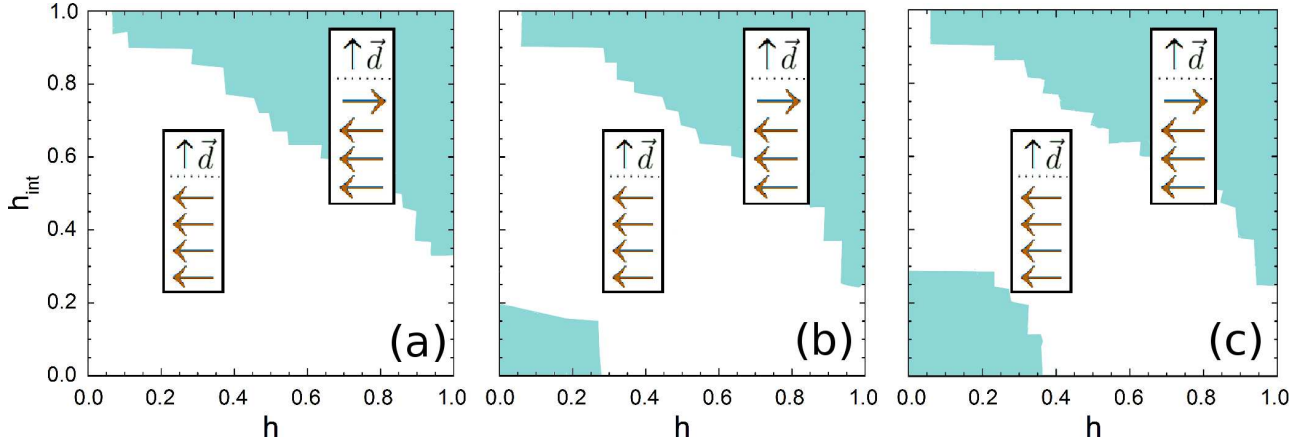


FIG. 8. (color online) phase diagrams for the energetically most favorable configuration in the plane (h_{int}, h) for $V = 0.0t$ (a), $V = -2.0t$ (b) and $V = -2.5t$ (c). The ferromagnetic exchange fields are expressed in units of the exchange amplitude $h_{\text{HM}} \cong 3.15$ corresponding to the transition value to an half-metal FM, where namely the density of the spin minority carriers goes to zero. The sketch represents the most favorable configurations with parallel (white area) and anti-parallel (blue area) interface-bulk magnetic moments alignment, respectively.

0.48, the optimal orientation at the interface is at an angle $\rho \approx 3\pi/8$ when the bulk magnetization is parallel to the \vec{d} -vector (i.e. $\theta = 0$). The angle ρ corresponding to the relative minimum of the Gibbs free energy moves from about $3\pi/8$ to $\pi/2$ when θ varies from 0 to $\pi/2$ (see Fig. 7 (f)). Interestingly, the minimum of the order parameter energy E_{op} , corresponding to the maximal variation of the gap amplitude, occurs always at $\rho = -\pi/2$ for any value of θ if we exclude the $\theta = 0$ configuration where $\pm\pi/2$ are degenerate in energy due to symmetry reasons. The comparison between the variation of the Gibbs energy ΔG and the order parameter energy ΔE_{op} clearly indicates a competition between a contribution due to the change of the order parameter in the TSC region, and consequently of the condensation energy, and another one related to the magnetic energy close to the interface.

B. Phase Diagram

The analysis of the Gibbs energy profile indicates that the ground state is not unique but depends on the strength of the exchange field. Therefore it is interesting to calculate the complete phase diagram in terms of h and h_{int} by evaluating the absolute minimum of the Gibbs free energy in the $[\theta, \rho]$ landscape. Furthermore, in order to assess the role of the superconducting correlations strength in determining the most stable magnetic configuration, we have also computed the phase diagram at different values of the attractive interaction for the TSC.

The results are reported in Fig. 8. They show that the parallel and antiparallel interface-bulk alignment of the magnetization lying on the (xy) -plane are the two most

stable configurations. The antiparallel state is favored for weak and strong ferromagnet while the parallel one is preferred at intermediate exchange values. A first order transition occurs at the boundary between the two regions of stability. Another consequence of the performed analysis is that the extension of the region for the antiparallel stability depends on the strength of the superconducting pairing coupling. This finding underlines the role of the superconducting state in modifying the magnetic configuration of the ferromagnet. Finally the boundaries of the antiparallel bulk-interface configuration for strong ferromagnet regime are only slightly affected in the direction of shrinking the region of stability for the parallel magnetic state. Indeed, in this case the antiparallel configuration is already preferred without the superconductivity and the ferromagnetic exchange field is dominant in the proximity effect.

It is worth pointing out that there is an asymmetry in the role played by the interface and the bulk exchange field which can be emphasized by scanning the phase diagram along lines with given h_{int} and h . Indeed at small fixed values of h_{int} ($\lesssim 0.2$) there is no reentrant behavior as a function of h while one does find the double transition for the antiparallel configuration in the case of small fixed values of h by tuning the amplitude of h_{int} . Such asymmetry underlines the role of the interfacial spin-dependent scattering in driving the reentrant behavior from the parallel to the antiparallel configuration in the regime where the magnetization at the interface is large with a small density of spin-minority electrons.

C. Density of States

To get a deeper understanding of the modification on the energy spectrum induced by the interface-bulk misalignment we evaluate the density of states (DoS) $\rho(i_z, \omega)$ at each layer within the FM and TSC region of the heterostructure. To do that, we analyze the integrated quantity $I(i_z) = \int_{-D}^0 \omega \rho(i_z, \omega) d\omega$, representing the contribution to the Gibbs energy coming from the electronic spectrum, with $-D$ being the lowest occupied energy level and 0 the effective Fermi energy for the system after the Bogoliubov rotation.

In Fig. 9 we report the spatial evolution of the difference $\Delta I = I(\overset{\rightarrow}{\leftarrow}) - I(\overset{\rightarrow}{\rightarrow})$ between the values of $I(i_z)$, corresponding to the antiparallel (i.e. $\rho = \pm\pi/2$ and $\theta = \mp\pi/2$) and the parallel (i.e. $\rho = \theta = \pi/2$) configurations, as a function of the ferromagnetic exchange field, assuming that $h = h_{\text{int}}$. Since $I(i_z)$ is a negative quantity, a positive ΔI indicates that the electronic spectrum contribution tends to favor the parallel configuration and the opposite for negative amplitudes. The analysis of the DoS reveals a significant dependence of the contribution $I(i_z)$ on the magnetic configuration and on the strength of the ferromagnetic exchange field. As shown in Fig. 9, the main change in the DoS occurs at the FM layers which are close to the interface. This reflects the scale length where the energy spectrum reconstruction mainly occurs.

In the TSC region the electronic reconstruction always favors the antiparallel state, as it is also expected from the evaluation of the order parameter energy E_{op} . Thus, no significant renormalization of the DoS close to the Fermi energy happens that interferes with the role of the order parameter in the energy balance.

In the FM side the energy contribution due to the electronic spectrum is highly nontrivial. For small values of the ferromagnetic exchange field there is an appreciable difference between the energy related to the electronic spectrum of the two magnetic configurations. Such difference becomes larger and larger in favor of the parallel configuration when h increases from 0.32 to 0.51. Then the difference decreases until the antiparallel configuration starts to dominate. The results of the DoS confirm a scenario of electronic modification close to the interface playing a significant role in the magnetic configuration transition.

It is worth pointing out that the modifications of the DoS are substantial both in the energy range of the superconducting gap and also outside it. This is partially due to the superconducting correlations and in part to the change of the DoS due to the processes of scattering at the interface at energies which are larger than the superconducting gap in the presence of exchange field split Fermi surfaces. Interestingly, in the regime of intermediate ferromagnetic exchange field, i.e. for h in the range

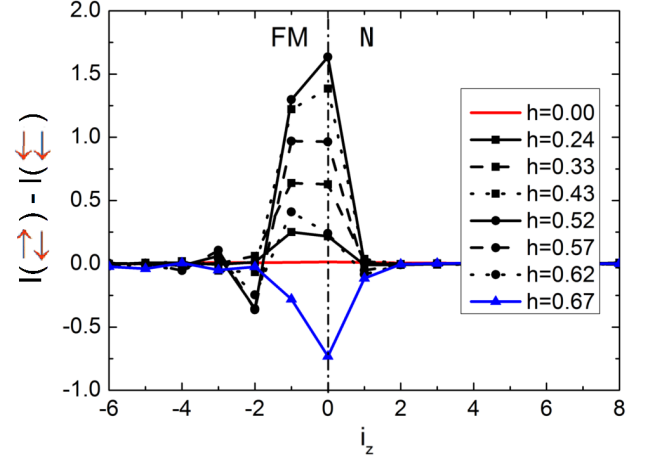


FIG. 9. (color online) difference of the integrated density of states for the antiparallel and the parallel configuration as a function of the layer position and of the exchange field strength for the FM-N interface. We consider an equal amplitude of the exchange field at the interface and in the bulk, i.e. $h = h_{\text{int}}$.

of 0.32 to 0.57, the density of states of the ferromagnetic layers close to the interface exhibits new electronic states close to the Fermi energy when the antiparallel configuration is considered. Although such states may represent a distinctive feature of the FM-TSC heterostructure, they do not contribute significantly in determining the stability of the ferromagnetic profile.

V. SPIN-POLARIZED PAIR CORRELATIONS

In this section we analyze the induced spin-triplet pair correlations, as defined in Eq. 4, with p_x and p_y orbital symmetry but having parallel $\uparrow\uparrow$ and $\downarrow\downarrow$ spin configuration along the z direction as compared to the state with zero spin projection associated with the bulk order parameter, i.e. the superposition $\uparrow\downarrow + \downarrow\uparrow$. These pair correlations are identically zero in the bulk, since the superconductor has no net spin polarization. However, it is possible to induce spin polarized pair correlations close to the interface, since a magnetization that is noncollinear to the \vec{d} -vector can lead to spin-flip processes and, then, to a consequent spin-mixing. It is instructive to consider the case of an uniform ferromagnet i.e., $\rho = \theta$, with a magnetization forming an angle θ with respect to the \vec{d} -vector. We show in Fig. 10 the spatial profile of the $F_{p_x}^{\sigma\sigma}(i_z)$ z -spin polarized pair correlations for both cases $\sigma = (\uparrow, \downarrow)$ and for different orientations of the magnetization.

As one can note, a magnetization parallel to the \vec{d} -vector ($\theta = 0$) does not induce z -spin polarized pair correlations. This can be understood by observing that to

contribute in the $F_{p_x}^{\sigma\sigma}(i_z)$ amplitude, the incident electrons and the scattered holes have to be spin polarized along the same z -direction and this can occur only when the Andreev reflection involves a change in the spin orientation because of the spin symmetry of the superconducting order parameter, as depicted in Fig. 11(a). Therefore, the resulting pair correlations have no contributions in the z -spin polarized pairing channel.

By changing the exchange field orientation from the direction perpendicular to the (xy) -plane (i.e. $\theta = 0$) to the in-plane ($\theta = \pi/2$), the amplitude of the z -spin polarized pair correlations exhibits a nonmonotonous behavior. They increase upon a critical angle $\theta_{max} \sim \pi/4$ and then decrease when the exchange field tends to point within the (xy) -plane. The appearance of nonzero correlations for the z -spin polarized pairs when the exchange field is not parallel to the \vec{d} -vector can be addressed by analyzing the process depicted in Fig. 11(b). The noncollinearity between the exchange field and the spin polarization of the incident electrons (holes) allows for a spin flip of the Andreev reflected holes (electrons) and therefore generates electron (hole) pairs with parallel spin orientation along the z -direction. More specifically, we note that the amplitude of the z -spin polarized pair correlations is maximum for angles close to $\theta \sim \pi/4$. Indeed, those orientations optimize the number of incident particles with spin polarization parallel to z together with the exchange amplitude for the mechanism of spin-flip process (i.e. the h_x component of the exchange field). On the other hand, the pairing amplitude is minimum when the magnetization lies in the plane, i.e. at $\theta = \pi/2$. This is because, in this case, although the amplitude of the exchange field is maximally active as a spin flip generator, the number of incident particles with spin polarization parallel to z is minimum.

We also find that the evolution of the pair correlations in the FM side is decaying and oscillating as a function of the layer position with the same period of those associated with the bulk order parameter (see for comparison the Fig. 2). Since there is always an energy split between the Fermi energies of electrons with spin up and down polarization at any orientation of the magnetization, we do expect a spatial dependence with an oscillating behavior. Indeed, the z -spin polarized pairs along the z direction get experience of the transverse component of the exchange field that is nonvanishing at any angle θ which is different from zero. Such component acts as a pair breaking term and makes the pairs acquiring a finite momentum which results in a spatial modulation of the pairing amplitude. Moreover, it is interesting to see that in the TSC side z -spin polarized pairs are also induced by a sort of inverse proximity effect, i.e. due to the penetration of the magnetization in the superconducting layers. Therefore, in the case of the existence of a pairing potential component $V^{\sigma\sigma}$, there would be a rotation of the \vec{d} -vector that can have significant consequences on the electronic transport in a Josephson junction configuration⁴⁸. Still,

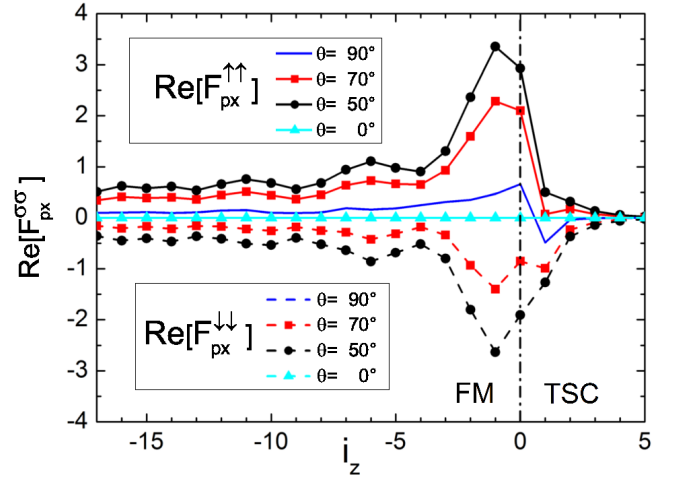


FIG. 10. (color online) Spatial variation of the real part of $F_{p_x}^{\uparrow\uparrow}$ and $F_{p_x}^{\downarrow\downarrow}$ pair correlations associated with the $\uparrow\uparrow$ (solid lines) and $\downarrow\downarrow$ (dashed line) spin-triplet configurations for a representative case of p_x orbital symmetry as a function of the magnetization direction θ and at a given exchange field $h = 0.16$. The amplitude of the correlator is scaled to the value of the bulk one $\text{Re}[F_{p_x}]$ in the $\uparrow\downarrow$ spin configuration. The FM-TSC interface is denoted by the dashed line.

the modulation of the pair correlator does not lead to a phase change as a function of the spatial coordinate.

A change in the amplitude of the ferromagnetic exchange field does not modify the general trend obtained for the case of $h = 0.16$. In particular, by increasing the ferromagnetic exchange one gets a reduction of the z -spin polarized triplet correlations. This is because the overall amplitude is set by the magnitude of the correlator associated with the superconducting order parameter. Taking into account the mechanisms presented in Fig. 11(b) one can also argue that the presence of a spin-flip process at the interface allows to generate z -spin polarized pairs even for the case of a bulk magnetization parallel to the \vec{d} -vector. For the other cases, we might expect that the interface-bulk misalignment tends to modify the amplitude of the z -spin polarized pair correlations close to the interface in a way that depends on the balance between the number of incident electrons and the effectiveness of the spin-flip generator. It is worth pointing out that, since the maximum amplitude of the z -spin polarized triplet correlations corresponds to an angle $\theta_{max} \sim \pi/4$, they do not have a relevant role in the balance of Gibbs free energy related to the proximity effect. On the other hand, in the case of an induced pair potential in the TSC region in the spin-polarize channel, due to a modification of the pairing glue at the interface, there would be a significant change of the energy balance related to the condensation energy.

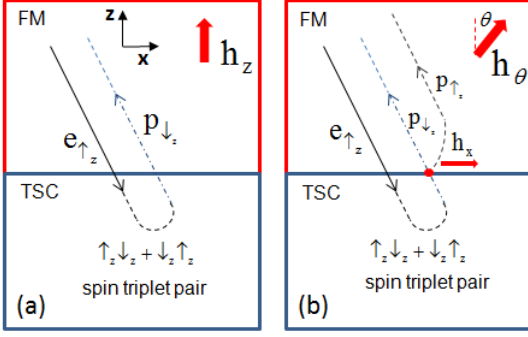


FIG. 11. (color online) Sketch of the Andreev processes that may contribute to the build up of the $F^{\uparrow\uparrow}$ and $F^{\downarrow\downarrow}$ z -spin polarized pair correlations. An electron ($e_{\uparrow z}$) with spin up aligned along the z direction can be scattered as a hole ($p_{\downarrow z}$) due to the spin symmetry of the triplet order parameter. (a) For a one-component exchange field which is parallel to the z -direction, the only allowed Andreev scattering is to convert an electron $e_{\uparrow z}$ into a hole $p_{\downarrow z}$ with opposite spin orientation. (b) For an exchange field aligned along a given direction θ (the magnetization has component along x and z) it is possible to inject an electron $e_{\uparrow z}$ with spin up along z and to get an Andreev reflected hole with opposite spin $p_{\downarrow z}$ or with the same spin polarization of the incident particle $p_{\uparrow z}$ due to the effect of the transverse h_x component to yield a spin-flip. This process allows to have z -spin polarized pair correlations along the z direction.

VI. DISCUSSION

In this section we would like to present a qualitative physical scenario related to the origin of the competing ground states in the FM-TSC heterostructure in the presence of spin-active interface processes.

We firstly consider the origin of the competition between the parallel and the antiparallel magnetic configurations within the FM-N heterostructure. To such purpose, we provide a simplified picture to justify the stability of a parallel bulk-interface state in the weak-intermediate ferromagnet and of an antiparallel one in the strong ferromagnet regime.

In the latter case, it is useful to consider the modification of the wave function in the ferromagnetic region close to the interface. We can schematically discuss this physical situation by means of a scattering formulation. Assuming that the interface plays the role of a spin-dependent barrier it is possible to determine the probability of an electron, propagating through the bulk with a given spin-direction and momentum, to be reflected or transmitted across the barrier. By solving the scattering problem, as expected the probability of reflection of a scattering electron increases as a function of the barrier potential strength Z .

Hence, an incident electron in the spin-majority band of the FM has experience of a larger (smaller) potential

barrier if the magnetization at the interface is not parallel to its spin, which leads to a smaller (larger) spin-filtering effect. Still, for the antiparallel configuration, the spin-minority electrons, having a spin-polarization parallel to the magnetization at interface, have a higher probability to be transmitted. The resulting overall effect is to have more electrons reflected in the spin-majority band as well as more electrons transmitted in the spin-minority band, respectively. Thus, there is an increase of the spin polarization close to the interface because the wave-function has a larger (smaller) density probability for the spin majority electrons in the antiparallel (parallel) bulk-interface magnetic state. Such an increase of the spin-density would correspond to a higher magnetization and consequently to a larger gain in the magnetic energy. Finally, it is interesting to observe that by computing the spin-dependent reflection and transmission probabilities for the weak ferromagnet regime, the processes become almost equivalent thus making more difficult to distinguish between the spin-polarization modification at the interface for the parallel and the antiparallel configurations. Then, the mechanism of wave-function reconstruction gets not effective in such regime.

In order to understand the origin of the antiparallel bulk-interface ground state in the phase diagram of the FM-N heterostructure for a weak ferromagnet, it is useful to analyze the problem by reducing the model to only two layers, i.e. the interface layer and its first neighbor (respectively $i_z=0$ and $i_z = -1$ in the notation of the heterostructure) for the two magnetic configurations. Assuming a collinear configuration, we consider the change of the energy spectrum due to the hybridization of the bands with the same spin polarization (the non collinear case does not change the results qualitatively). For the parallel configuration the spin polarized energy bands get split by the interlayer hopping and in the limit of $h = h_{\text{int}}$ they are given by $E_{\sigma}^P = \epsilon(k) - \sigma(h * M + t_{\perp})$. The expression for E_{σ}^P is obtained by assuming the same in-plane spectrum within the layer at $i_z = 0$ and -1 , and the index $\sigma = 1(-1)$ labels the spin majority (minority) electrons in the bulk FM. For the antiparallel configuration the energy spectrum is split as a square root of the interlayer hopping, i.e. we have $E_{\sigma}^{AP} = \epsilon(k) - \sigma \sqrt{(h * M)^2 + t_{\perp}^2}$. By comparing the energy spectra for the two magnetic configurations for the spin-majority channels, one can deduce that for small exchange fields the energy gain is larger for the parallel configuration if compared to the antiparallel one because of the linear correction in the energy spectrum.

We conclude that for weak-intermediate ferromagnets the parallel bulk-interface magnetic configuration is the most energetically favored state because of the energy spectrum reconstruction. On the other hand, in the regime of strong ferromagnetic exchange field, it is the wave function reconstruction that primarily drives the stability of the antiparallel configuration. We finally note that, for the FM-N heterostructure, the invariance of the Hamiltonian under spin rotation makes all the magnetic

orientations degenerate in energy. These conclusions have been drawn for a physical situation with collinear magnetization. Similar arguments apply also for the case of a noncollinear bulk-interface configuration.

We focus now on discussing the reasons for having the spin-triplet superconductor to favor an antiparallel bulk-interface magnetic state with a planar spin orientation (i.e. perpendicular to the \vec{d} -vector) at any given strength of the ferromagnetic exchange field. We recall that this behavior can be deduced by the observation of the profile for the pairing energy E_{op} which is always minimized when the magnetization in the bulk and at the interface lies in the plane perpendicular to the \vec{d} -vector and are aligned with opposite spin orientations. Since the E_{op} energy is directly related to the amplitude of the order parameter in the superconducting region, it is relevant to analyze the intensity and the character of the Andreev processes. It is well known that the Andreev reflection amplitude enters plays a role in this context because it is the probability of an electron (hole) injected from the ferromagnet to be reflected as hole (electron), thus providing the intensity for the creation (annihilation) of an electrons (holes) pair in the superconductor. Then the Andreev scattering amplitude sets the strength of the pair fluctuations in the superconductor close to the interface and thus it is the main effect in driving the modification of the pair amplitude. Based on the nature of this process, we can argue that a large value of the Andreev reflection amplitude at the FM-TSC interface would then result into a significant reduction of the pair amplitude and in turn of the superconducting order parameter in the TSC region close to the interface.

Among all the Andreev processes, those related to the creation (annihilation) of an electrons pair with a different phase are of particular relevance because they interfere destructively when they sum up in the formation of the pairing amplitude. From a general point of view, such non-trivial signs in the Andreev scattering can originate from the orbital dependence of the superconducting order parameter or they can be due to spin-dependent phase shifts for the mismatch in the magnetic configuration between the superconductor and the ferromagnet. A distinct and limiting case occurs in the presence of bound states at the interface where the Andreev probability is maximized for the correspondent energy of the incident electron (hole). The relation between the Andreev processes and the pairing amplitude variation has been shown to hold for a d -wave superconductor interfaced to the vacuum where bound states occur at specific orientations of the interface with respect to the d -wave nodal directions. There, a maximal reduction of the order parameter is observed when the orientation of the interface is such to have Andreev bound states in the density of states⁵⁶.

As mentioned in the Section III, for the case of a spin-triplet superconductor and for the examined layered geometry in this paper, the chiral orbital symme-

try does not lead to Andreev scattering processes that involve sign changes in the pairing potential along the particle-hole trajectories. Hence, we expect that the modifications of the order parameter should be mainly ascribed to the contributions of spin-dependent scattering. Taking into account the results for the homogeneous ferromagnet⁴⁷⁻⁴⁹, we are aware that the pair fluctuations are suppressed when the magnetization of the ferromagnet lies in the plane of the spin of the Cooper pairs, i.e. E_{op} is maximal for a magnetization which is perpendicular to the \vec{d} -vector. This is because in such a configuration there are no phase shifts in the Andreev processes⁴⁷. Considering now the competition between the other possible inequivalent configurations, i.e. the parallel and the antiparallel bulk-interface magnetic states, we observe that, in general and in the absence of bound states, the amplitude of the Andreev scattering decrease as a function of the barrier potential strength⁵⁷. We note again that in the antiparallel configuration the incident electron in the spin-majority band gets experience of a greater barrier potential if compared to case of parallel spin-polarization. Such observation would imply that the intensity of the Andreev scattering probability is smaller for the antiparallel bulk-interface magnetic state than for the parallel one therefore that the pairing amplitude is less affected by the scattering processes and thus less reduced. This qualitative argument would support the results of having a larger gain in the condensation energy when the bulk-interface magnetizations are antiparallel oriented. We also note that the discussed mechanism is consistent with the fact that there is a weak dependence on the strength of the ferromagnetic exchange field.

VII. CONCLUSIONS

We have studied the physical behavior of a ferromagnet- spin-triplet superconductor heterostructure with a layered geometry assuming an orbital chiral symmetry for the superconducting order parameter and spin dependent scattering at the interface. By means of a self-consistent approach on a three-dimensional lattice we have determined the spatial profile of the pairing amplitude and magnetization in terms of the strength of the ferromagnetic exchange field and the spin-active processes at the interface. We find that the pairing amplitude in the TSC region close to the interface increases if the magnetization moves from being parallel to perpendicular to the \vec{d} -vector. In the presence of a spin-active interface a configuration with in-plane antialigned magnetic moments for the bulk-interface layers maximizes the value of the pairing amplitude. As expected, the penetration of the Cooper pairs in the FM leads to induced pairing amplitudes with zero-spin projection that we show to have a damped oscillating behavior if the magnetization is out-of-plane, while it is monotonously decaying when the magnetization is perpendicular to the \vec{d} -vector, i.e. parallel to the spin

direction of the Cooper pairs. A distinctive feature is the oscillating behavior of the proximity effect which brings a phase change only if the angle between the magnetization and the \vec{d} -vector is in the $\sim [0, \pi/4]$ window. The spin-active scattering mainly modifies the behavior close to the interface by influencing the intensity and the phase change of the pairing amplitude. One of our main results has been to show that spin-polarized pair correlations are also induced both at the interface in the TSC and with a long range penetration length in the FM if the magnetization is noncollinear to the \vec{d} -vector. We have shown that their amplitude is maximized at an angle $\theta \sim \pi/4$ for a uniform ferromagnet and it has a non trivial behavior in the presence of a bulk-interface magnetic misalignment. We have pointed out that such correlations can play a major role in the case of the existence of a pair potential in the same spin channel at the interface of the spin-triplet superconductor. This effect can lead to a re-orientation of the \vec{d} -vector approaching the ferromagnet and drastically influence the anisotropy of the ferromagnet as well as the charge and spin transport of the hybrid structure⁴⁸.

The knowledge of the key physical quantities of the FM-N and FM-TSC hybrids has been used to provide the basis for a detailed analysis of the optimal magnetic configuration as due to the coupling with a spin-triplet superconductor. The study of the Gibbs free energy of the system reveals that the rotational spin invariance of the ferromagnet is generally broken due to the coupling with the superconductor and in turn the FM develops an anisotropy which favors an in-plane orientation of the magnetization. In the case of a uniform ferromagnet, we have demonstrated that the driving mechanism for the stabilization of the bulk-interface relative orientation of magnetization is based on the gain of the superconducting condensation energy rather than on the proximity effect. The presence of an active ferromagnetic layer at the interface leads to a different physical scenario. There are two optimal magnetic states which minimize the Gibbs free energy of the system: they have a parallel or antiparallel bulk-interface alignment with spin orientation degeneracy in the FM-N hybrid while with a magnetization oriented in the plane perpendicular to the \vec{d} -vector for the FM-TSC heterostructure. As our central result we have demonstrated, by exploring the full space of parameters as a function of the relative exchange field strength at the interface and in the bulk, that the system can switch between the two ground-state configurations. The antiparallel configuration

is generally favored for a regime of weak and strong ferromagnet otherwise the parallel state is stabilized. In the latter the spin dependence of the energy spectrum in the FM domain close to the interface cooperates with the energy contribution due to the modification of the superconducting order parameter which would always tend to favor an antiparallel interface-bulk magnetic configuration. We emphasize that such electronic structure effect has important contributions inside and outside the energy window of the superconducting gap. We have demonstrated that such effects lead to noncollinear bulk-interface magnetic configurations when the bulk magnetization is assumed fixed along a given direction and that at the interface can vary to minimize the Gibbs energy.

The results obtained in this paper represent a solid platform to investigate a FM-TSC hybrid in a conventional epitaxially grown geometry. We point out that they can be of direct interest for the case of the Sr_2RuO_4 spin-triplet superconductor interfaced with other ferromagnetic oxides having matching lattice parameters, i.e. SrRuO_3 or doped LaMnO_3 , but can also be indirectly used to extract information of the symmetry of the order parameter of unknown superconductors through the investigation of the magnetic profile in the ferromagnet. Indeed, the occurrence of magnetization anisotropy within the FM can be experimentally probed measuring the magnetic moment profile as a function of the layer position via nuclear magnetic resonance, muon spin rotation or polarized neutron reflectometry. The latter has been successfully applied, for instance, to observe a surprisingly large superconductivity-induced modulation of the ferromagnetic magnetization profile in superlattices made of high temperature superconductors interfaced with ferromagnetic manganites⁵⁵. Finally, since a spin-active interface plays a relevant role in determining the character of the spin-triplet pair correlations induced in the FM and in tuning the free energy profile, it is expected to be an important ingredient for possible spin-valve devices based on spin-triplet superconductors as well as for controlling the dynamical evolution of the magnetization in the ferromagnet.

ACKNOWLEDGMENT

The research leading to these results has received funding from the EU -FP7/2007-2013 under grant agreement N. 264098 - MAMA. M.C. and D.M. acknowledge support from the Short Term Mobility (STM) program of the Consiglio Nazionale delle Ricerche (CNR).

* Electronic address: d.terrade@fkf.mpg.de

¹ I. Zutic, J. Fabian, and S. Das Sarma, Rev. Mod. Phys. **76**, 323 (2004).

- ² A. I. Buzdin, Rev. Mod. Phys. **77**, 935 (2005).
- ³ F.S. Bergeret, A.F. Volkov, and K.B. Efetov, Rev. Mod. Phys. **77**, 1321 (2005).
- ⁴ M. Eschrig and T. Lofwander, Nature Physics **4**, 138 (2008).
- ⁵ P. Fulde and R. A. Ferrell, Phys. Rev. **135**, A550 (1964); A. I. Larkin and Yu. N. Ovchinnikov, Zh. Eksp. Teor. Fiz. **47**, 1136 (1964) [Sov. Phys. JETP **20**, 762 (1965)].
- ⁶ M. Cuoco, P. Gentile, C. Noce, Phys. Rev. Lett. **91**, 197003 (2003); Z.-J. Ying, M. Cuoco, C. Noce, and H.-Q. Zhou, Phys. Rev. B **74**, 012503 (2006).
- ⁷ E. A. Demler, G. B. Arnold, and M. R. Beasley, Phys. Rev. B **55**, 15174 (1997).
- ⁸ Z. Radovic, M. Ledvij, L. Dobrosavljevic-Grujic, A. I. Buzdin, J. R. Clem, Phys. Rev. B **44**, 759 (1991).
- ⁹ J. S. Jiang, D. Davidovic, D. H. Reich, and C. L. Chien, Phys. Rev. Lett. **74**, 314 (1995).
- ¹⁰ V.V. Ryazanov *et al.*, Phys. Rev. Lett. **86**, 2427 (2001).
- ¹¹ M. G. Khusainov and Y. N. Proshin, Phys. Rev. B **56**, R14283 (1997).
- ¹² Y.V. Fominov, N. M. Chtchelkatchev, and A. A. Golubov, Phys. Rev. B **66**, 014507 (2002).
- ¹³ K. Halterman and O. T. Valls, Phys. Rev. B **70**, 104516 (2004).
- ¹⁴ F.S. Bergeret, A.F. Volkov, and K.B. Efetov, Phys. Rev. Lett. **86**, 3140 (2001).
- ¹⁵ F.S. Bergeret, A.F. Volkov, and K.B. Efetov, Phys. Rev. B **68**, 064513 (2003).
- ¹⁶ T. Lofwander, T. Champel, J. Durst, M. Eschrig, Phys. Rev. Lett. **95**, 187003 (2005).
- ¹⁷ K. Halterman, P. H. Barsic, and O. T. Valls, Phys. Rev. Lett. **99**, 127002 (2007).
- ¹⁸ Y. Asano, Y. Tanaka and A. A. Golubov, Phys. Rev. Lett. **98**, 107002 (2007).
- ¹⁹ V. Braude and Yu. V. Nazarov, Phys. Rev. Lett. **98**, 077003 (2007).
- ²⁰ T. Yokoyama, Y. Tanaka and A.A. Golubov, Phys. Rev. B **75**, 134510 (2007).
- ²¹ J. Linder, T. Yokoyama, A. Sudbo and M. Eschrig, Phys. Rev. Lett. **102**, 107008 (2009).
- ²² J. Linder, A. Sudbo, T. Yokoyama, R. Grein and M. Eschrig, Phys. Rev. B **81**, 214504 (2010).
- ²³ R. S. Keizer, S. T. B. Goennenwein, T. M. Klapwijk, G. Miao, G. Xiao, and A. Gupta, Nature (London) **439**, 825 (2006).
- ²⁴ I. Sosnin, H. Cho, V. T. Petrashov, and A. F. Volkov, Phys. Rev. Lett. **96**, 157002 (2006).
- ²⁵ T. S. Khaire, M. A. Khasawneh, W. P. Pratt Jr., and N. O. Birge, Phys. Rev. Lett. **104**, 137002 (2010).
- ²⁶ J.W. A. Robinson, J. D. S. Witt, and M. G. Blamire, Science **329**, 59 (2010).
- ²⁷ D. Sprungmann, K. Westerholt, H. Zabel, M. Weides, and H. Kohlstedt, Phys. Rev. B **82**, 060505 (2010).
- ²⁸ M. S. Anwar, F. Czeschka, M. Hesselberth, M. Porcu, and J. Aarts, Phys. Rev. B **82**, 100501 (2010).
- ²⁹ C. Klose *et al.*, Phys. Rev. Lett. **108**, 127002 (2012).
- ³⁰ J. Linder, T. Yokoyama and A. Sudbo, Phys. Rev. B **79**, 054523 (2009).
- ³¹ Ya. V. Fominov, *et al.*, JETP Letters **91**, 308 (2010).
- ³² S. Oh, D. Youm, and M. R. Beasley, Appl. Phys. Lett. **71**, 2376 (1997).
- ³³ T. Y. Karminskaya, A. A. Golubov, and M. Y. Kupriyanov, Phys. Rev. B **84**, 064531 (2011).
- ³⁴ J. Zhu, I. N. Krivorotov, K. Halterman, and O. T. Valls, Phys. Rev. Lett. **105**, 207002 (2010) and references therein.
- ³⁵ H. Tou *et al.*, Phys. Rev. Lett. **77**, 1374 (1996); H. Tou *et al.*, Phys. Rev. Lett. **80**, 3129 (1998).
- ³⁶ S. S. Saxena, P. Agarwal, K. Ahilan, F. M. Grosche, R. K. W. Haselwimmer, M. J. Steiner, E. Pugh, I. R. Walker, S. R. Julian, P. Monthoux, G. G. Lonzarich, A. Huxley, I. Sheikin, D. Braithwaite, and J. Flouquet, Nature **406**, 587 (2000).
- ³⁷ I. J. Lee, M. J. Naughton, G. M. Danner, and P. M. Chaikin, Phys. Rev. Lett. **78**, 3555 (1997); J. I. Oh and M. J. Naughton, Phys. Rev. Lett. **92**, 067001 (2004).
- ³⁸ Y. Maeno, H. Hashimoto, K. Yoshida, S. Nishizaki, T. Fujita, J. G. Bednorz, and F. Lichtenberg, Nature **372**, 532 (1994); A. P. Mackenzie and Y. Maeno, Rev. Mod. Phys. **75**, 657 (2003).
- ³⁹ G.M. Luke *et al.*, Nature **394**, 558 (1998).
- ⁴⁰ E. Bauer *et al.*, Phys. Rev. Lett. **92**, 027003 (2004).
- ⁴¹ H. Q. Yuan *et al.*, Phys. Rev. Lett. **97**, 017006 (2006).
- ⁴² L. P. Gorkov and E. I. Rashba, Phys. Rev. Lett. **87**, 037004 (2001).
- ⁴³ Y. Krockenberger *et al.*, Appl. Phys. Lett. **97**, 082502 (2010).
- ⁴⁴ A. P. Mackenzie and Y. Maeno, Rev. Mod. Phys. **75**, 657 (2003).
- ⁴⁵ G. Annunziata, M. Cuoco, C. Noce, A. Sudbo, and J. Linder, Phys. Rev. B **83**, 060508(R) (2011).
- ⁴⁶ P. M. R. Brydon and D. Manske, Phys. Rev. Lett. **103**, 147001 (2009); B. Bujnowski, C. Timm, and P. M. R. Brydon, J. Phys.: Condens. Matter **24**, 045701 (2012).
- ⁴⁷ P. M. R. Brydon, Phys. Rev. B **80**, 224520 (2009).
- ⁴⁸ P. M. R. Brydon, Y. Asano, and C. Timm, Phys. Rev. B **83**, 180504 (2011).
- ⁴⁹ P. Gentile, M. Cuoco, A. Romano, C. Noce, D. Manske, and P. Brydon, arXiv:1208.5871.
- ⁵⁰ J. Linder, M. Cuoco, and A. Sudbo, Phys. Rev. B **81**, 174526 (2010).
- ⁵¹ K. Kuboki and H. Takahashi, Phys. Rev. B **70**, 214524 (2004).
- ⁵² M. Cuoco, A. Romano, C. Noce, and P. Gentile, Phys. Rev. B **78**, 054503 (2008).
- ⁵³ K. Kuboki, J. Phys. Soc. Jap. **70**, 2698 (2001).
- ⁵⁴ L. J. Buchholtz and G. Zwicknagl, Phys. Rev. B **23**, 5788 (1981); C. Bruder, Phys. Rev. B **41**, 4017 (1990).
- ⁵⁵ J. Hoppler *et al.*, Nat. Mat. **8**, 315 (2009).
- ⁵⁶ S. Kashiwaya and Y. Tanaka, Rep. Prog. Phys. **63**, 1641 (2000).
- ⁵⁷ G. E. Blonder, M. Tinkham and T. M. Klapwijk, Phys. Rev. B **25**, 4515 (1982).